Atmos. Chem. Phys. Discuss., 15, 19873–19902, 2015
www.atmos-chem-phys-discuss.net/15/19873/2015/
doi:10.5194/acpd-15-19873-2015


Atmospheric Chemistry and Physics Discussions



# Plant surface reactions: an ozone defence mechanism impacting atmospheric chemistry

**W. Jud[1], L. Fischer[1], E. Canaval[1], G. Wohlfahrt[2,3], A. Tissier[4], and A. Hansel[1]**

[1]Institute of Ion and Applied Physics, University of Innsbruck, 6020 Innsbruck, Austria
[2]Institute of Ecology, University of Innsbruck, 6020 Innsbruck, Austria
[3]European Academy of Bolzano, 39100 Bolzano, Italy
[4]Leibniz Institute of Plant Biochemistry, Department of Cell and Metabolic Biology, 06120 Halle, Germany

Received: 3 June 2015 – Accepted: 22 June 2015 – Published: 21 July 2015

Correspondence to: A. Hansel (armin.hansel@uibk.ac.at)

Published by Copernicus Publications on behalf of the European Geosciences Union.







## Abstract

Elevated tropospheric ozone concentrations are considered a toxic threat to plants, responsible for global crop losses with associated economic costs of several billion dollars per year. Plant injuries have been linked to the uptake of ozone through stomatal pores and oxidative damage of the internal leaf tissue. But a striking question remains: how much ozone effectively enters the plant through open stomata and how much is lost by chemical reactions at the plant surface?

In this laboratory study we could show that semi-volatile organic compounds exuded by the glandular trichomes of different *Nicotiana tabacum* varieties are an efficient ozone sink at the plant surface. In our experiments, different diterpenoid compounds were responsible for a strongly variety dependent ozone uptake of plants under dark conditions, when stomatal pores are almost closed. Surface reactions of ozone were accompanied by prompt release of oxygenated volatile organic compounds, which could be linked to the corresponding precursor compounds: ozonolysis of *cis*-abienol ($C_{20}H_{34}O$) – a diterpenoid with two exocyclic double bonds – caused emissions of formaldehyde (HCHO) and methyl vinyl ketone ($C_4H_6O$). The ring-structured cembratrien-diols ($C_{20}H_{34}O_2$) with three endocyclic double bonds need at least two ozonolysis steps to form volatile carbonyls such as 4-oxopentanal ($C_5H_8O_2$), which we could observe in the gas phase, too.

Fluid dynamic calculations were used to model ozone distribution in the diffusion limited leaf boundary layer under daylight conditions. In the case of an ozone-reactive leaf surface, ozone gradients in the vicinity of stomatal pores are changed in such a way, that ozone flux through the open stomata is strongly reduced.

Our results show that unsaturated semi-volatile compounds at the plant surface should be considered as a source of oxygenated volatile organic compounds, impacting gas phase chemistry, as well as efficient ozone sink improving the ozone tolerance of plants.






ACPD
15, 19873–19902, 2015



## 1 Introduction

Tropospheric ozone ($O_3$) is formed as a product of photochemical reactions involving nitrogen oxides ($NO_x$) and volatile organic compounds (VOC) as precursors (Jenkin and Clemitshaw, 2000). Increasing anthropogenic precursor emissions from fossil fuel and biomass burning have led to elevated ambient ozone concentrations over large portions of the earth's surface. Today, many regions experience near surface ozone background levels greater than 40 parts per billion volume (ppbv) (Vingarzan, 2004), levels which may be responsible for cellular damage inside leaves (Hewitt et al., 1990; Wohlgemuth et al., 2002) adversely affecting photosynthesis and plant growth (Ashmore, 2005). Toxic ozone concentrations cause visible leaf injury, plant damage and reduction in crop yields with associated economic costs of several billion dollars per annum worldwide (Wang and Mauzerall, 2004; Van Dingenen et al., 2009). Tropospheric ozone concentrations are expected to rise significantly through the next century especially during warm seasons, increasing the hazard of ozone damage to vegetation (Dentener et al., 2006; Sitch et al., 2007).

Traditionally, the risk of ozone damage to plants is estimated on the basis of the accumulated ozone exposure above 40 ppbv (AOT 40) (Felzer et al., 2005). However, the negative effects of ozone on vegetation are more closely related to the effective dose, i.e. the stomatal flux × time minus the portion of ozone which can be detoxicated by the plant defence system (Massman, 2004).

Accurate experimental quantification of the stomatal uptake of ozone is complicated by the presence of other ozone sinks, either in the gas phase or on the plant surface (Fruekilde et al., 1998; Cape et al., 2009). In previous studies the ozone flux through the stomata was calculated by multiplying the stomatal ozone conductance with the ambient ozone concentration (Kurpius and Goldstein, 2003; Cieslik, 2004; Goldstein et al., 2004; Fares et al., 2012), assuming similar gradient profiles of ozone and $H_2O$ close to the stomata. As we will show, in the case of ozone-reactive leaf surfaces this approach is not correct and leads to an overestimation of stomatal ozone uptake.





ACPD
15, 19873–19902, 2015



We present results from ozone fumigation experiments, in which intact leaves of different varieties of tobacco (*Nicotiana tabacum*) were exposed to elevated ozone levels (20–150 ppbv) under light and dark conditions in an exceptionally clean plant enclosure system (see Materials and methods section for experimental details). As is the case for many other plant species (Fahn, 1988), tobacco leaves possess glandular trichomes. In tobacco, various diterpenoids are the major compounds exuded by these secretory structures at the leaf surface (Sallaud et al., 2012). The exudates cover the plant leaves as a defence barrier, for example against arthropod pests (Wagner, 1991; Lin and Wagner, 1994); they were shown to have an anti-fungal (Kennedy et al., 1992) and insecticidal action (Kennedy et al., 1995). We show that a tobacco variety secreting the diterpenoid *cis*-abienol also has a very powerful chemical protection shield against stomatal ozone uptake due to ozone depletion at its leaf surface.

Surface-assisted ozonolysis not only protects plants from uptake of phytotoxic ozone through stomata, but also acts as a source of volatile carbonyls into the atmosphere, impacting atmospheric chemistry. To our knowledge, our study reports for the first time on detailed measurements of plant surface-assisted ozonolysis of semi-volatile diterpenoids forming volatile carbonyl products.

## 2 Materials and methods

### 2.1 Plant material

We used the following four tobacco cultivars: *Ambalema*, secreting only the diterpenoid *cis*-abienol ($C_{20}H_{34}O$, see Fig. 1), *BYBA* secreting $\alpha$- and $\beta$-cembratrien-diols (CBTdiols, $C_{20}H_{34}O_2$, see Fig. 1) and *Basma Drama*, secreting all these compounds (Sallaud et al., 2012). The new 3H02 line does not exude diterpenoids at all (see Appendix A).

Seeds of the tobacco cultivars were obtained from the Leibniz Institute of Plant Biochemistry, Department of Cell and Metabolic Biology, Halle. The plants were grown in





ACPD
15, 19873–19902, 2015



the green houses of the Institute of Ecology of the University of Innsbruck for 8–10 weeks in standard soil.

Before being used in the experiments the sample plants were allowed to adapt 1–4 weeks in the laboratory, obtaining light from the same true light lamp type as used during the measurements (see Setup section).

Plants were installed into the plant enclosure used for ozone fumigation the evening before the actual experiment, so they could adapt to the system and recover from possible stress during installation. The (single-sided) leaf area enclosed was typically in the range of 250–850 $cm^2$. The sample plants were well watered and in a good physiological condition ($CO_2$ fluxes during dark and light conditions are given in Table S1 in the Supplement) and showed no visible signs of damage. At the beginning of the experiments, when no ozone was added, no significant stress signals in form of green leaf volatiles were detected.

In total, combined dark and light ozone fumigation experiments were conducted with five *Ambalema*, two *Basma Drama*, one *BYBA* and three 3H02 samples. Moreover, experiments under solely light conditions were conducted with eight *Ambalema*, four *Basma Drama*, four *BYBA* and two 3H02 plants. Each sample plant was tested only once.

## 2.2 Setup

In the present ozone experiments we used only inert materials such as Teflon®, PEEK® or Duran® glass in order to minimise artificial side-reactions of ozone with unsaturated compounds, present in e.g. sealing materials like rubber. Moreover, special care was taken to avoid fingerprints, which could result in side reactions of ozone with skin oils (Wisthaler and Weschler, 2010). Ozone loss, estimated from measured ozone concentrations at the inlet and outlet of the empty plant enclosure, was typically less than 5 %.

For plant fumigation, synthetic air 5.0 grade was mixed with $CO_2$ 4.8 grade (both Messer Austria GmbH, Gumpoldskirchen, Austria). By bubbling the air in distilled water





ACPD
15, 19873–19902, 2015



and passing it by a subsequent thermoelectric cooler (TEC) the relative humidity was set. Before entering the plant enclosure, the air was flushed through an ozone generator (UVP, Upland (CA), USA). The enclosure system consisted of a desiccator (Schott Duran®) of 17.3 L volume, turned upside-down, and two end-matched PTFE® ground plates. A central hole served as feed-through for the plant stem, possible gaps were sealed with Teflon® tape.

An ozone detector (Model 49i, Thermo Fisher Scientific Inc. Franklin (MA), USA) and an infra-red gas analyser (LI-840A $CO_2/H_2O$ Analyzer, LI-COR® inc., Lincoln (NE), USA) were sampling at 2 min intervals from either the inlet or outlet of the enclosure. Plant enclosure inlet ozone concentrations were typically kept constant throughout each experiment and adjusted to obtain realistic ambient ozone concentrations at the enclosure outlet during light conditions (e.g. ∼ 60 ppbv in Fig. 2). Relative humidity in the plant enclosure ranged from typically ∼ 55 % in dark experiments up to ∼ 95 % in light experiments.

VOC were quantitatively detected at the enclosure outlet by a Selective Reagent Ionization Time-of-Flight Mass Spectrometer (SRI-ToF-MS, see next section) which was switched every 6 min between $H_3O^+$ and $NO^+$ reagent ion mode.

Sample plants were illuminated by a true light lamp (Dakar, MT/HQI-T/D, Lanzini Illuminazione, Brescia, Italy). Infra-red light was shielded off by a continuously flushed water bath in order to prevent heating of the plant enclosure. Photosynthetically active radiation (PAR) was measured with a sunshine sensor (model BF3, Delta T Devices Ltd, Cambridge, UK) and temperature on the outer plant enclosure surface with K-type thermocouples.

### 2.3 SRI-ToF-MS

The UIBK Advanced SRI-ToF-MS (University of Innsbruck Advanced Selective Reagent Ionization Time-of-Flight Mass Spectrometer, Breitenlechner and Hansel, 2015) combines the high mass resolution of PTR-ToF-MS (Graus et al., 2010) with





ACPD
15, 19873–19902, 2015



the capability to separate isomeric compounds having specific functional groups. For this purpose, the SRI-ToF-MS makes use of different chemical ionization pathways of a set of fast switchable primary ions (here: $H_3O^+$ and $NO^+$). Moreover, the employment of different primary ions could help to differentiate molecules suffering from fragmentation onto the same mass to charge ratio in the standard $H_3O^+$ mode (Karl et al., 2012).

Examples of differentiable isomers are aldehydes and ketones. In the $H_3O^+$ reagent ion mode, aldehydes and ketones both exhibit proton transfer and thus e.g. methyl vinyl ketone (MVK) and methacrolein (MACR) are both detected as $C_4H_7O^+$ ($m/z$ 71.050). In $NO^+$ reagent ion mode, most aldehydes exhibit hydride ion transfer and ketones clustering reactions, comparable to the ionization mechanisms in a SIFT instrument (Španěl et al., 1997). Thus MVK is detected as $C_4H_6O \cdot NO^+$ ($m/z$ 100.040), whereas MACR is detected as $C_4H_5O^+$ ($m/z$ 69.034).

In addition to isomeric separation, the high flow through the drift tube (here: ~ 500 mL min$^{-1}$ compared to 10–20 mL min$^{-1}$ in a standard instrument) allows for the first time the detection of semi-volatile compounds such as the diterpenoid *cis*-abienol ($C_{20}H_{34}O$).

The SRI-ToF-MS was operated under standard conditions, 60 °C drift tube temperature, 540 or 350 V drift voltage and 2.3 mbar drift pressure, corresponding to an $E/N$ of 120 or 78 Td ($E$ being the electric field strength and $N$ the gas number density; 1 Td = $10^{-17}$ V cm$^2$) in $H_3O^+$ respectively $NO^+$ reagent ion mode. The instrument was calibrated approximately once a week by dynamic dilution of VOC using 2 different gas standards (Apel Riemer Environmental Inc., Broomfield (CO), USA), containing ca. 30 different VOC of different functionality distributed over the mass range of 30–204 amu. Full SRI-ToF-MS mass spectra were recorded up to $m/z$ 315 with a 1 s time resolution. Raw data analysis was performed using the PTR-ToF Data Analyzer v3.36 and v4.17 (Müller et al., 2013).





ACPD
15, 19873–19902, 2015



## 2.4 *cis*-abienol identification

For the identification of *cis*-abienol a pure standard was acquired (Toronto Research Chemicals, Toronto, Canada). The powder was dissolved in n-hexane and applied on the surface of a glass container, which was put into the enclosure system and treated like the plant samples. In $H_3O^+$ reagent ion mode, the major *cis*-abienol derived signal was detected on $m/z$ 273.258 ($C_{20}H_{33}^+$); like many other alcohols, *cis*-abienol is losing $H_2O$ after the protonation reaction. Minor fragment signals in the range of a few percent were detected at $m/z$ 191.180 ($C_{14}H_{23}^+$), $m/z$ 163.149 ($C_{12}H_{19}^+$) and $m/z$ 217.196 ($C_{16}H_{25}^+$), respectively.

In $NO^+$ reagent ion mode, the major *cis*-abienol derived signals were detected at $m/z$ 272.250 ($C_{20}H_{32}^+$) and $m/z$ 178.172 ($C_{13}H_{22}^+$). Minor signals were measured at $m/z$ 163.149 ($C_{12}H_{19}^+$) and $m/z$ 134.101 ($C_{10}H_{14}^+$), respectively.

Ozonolysis of the pure *cis*-abienol standard yielded the same primary ozonolysis products (see below) as in the case of *Ambalema* plants.

## 2.5 Leaf stripping

In order to relate the observed ozonolysis carbonyls to plant surface reactions, leaf exudates of untreated tobacco plants were stripped off by dipping leaves (of similar area) of untreated *Ambalema*, *Basma Drama* and 3H02 plants into n-hexane (~ 100 mL for 1000 $cm^2$ leaf area) for ~ 1 min. The n-hexane – leaf exudate solution was then distributed as evenly as possible onto the inner surface of the empty desiccator serving as plant enclosure. n-hexane evaporated quickly and was further reduced by flushing the glass cuvette with pure synthetic air. Afterwards, ozone fumigation experiments were performed similar to the experiments with intact plants.





ACPD
15, 19873–19902, 2015



## 2.6 GC-MS analysis

Non-volatile ozonolysis products and unreacted surface compounds were analysed by GC-MS (see also Supplement). Directly after the ozone fumigation experiments we extracted leaf exudates and low volatility ozonolysis products from the fresh tobacco leaves (see Leaf Stripping section). 1 µL portions of the samples were then injected directly into a GC-MS for analysis on a 6890 N gas chromatograph coupled to a 5973 N mass spectrometer (Agilent Technologies) according to the procedures described elsewhere (Sallaud et al., 2012).

Tobacco diterpenoids were identified on the basis of their mass spectra, as described in the literature (Enzell et al., 1984).

## 2.7 Fluid dynamic calculations

In order to visualise the ozone concentration gradients caused by plant ozone uptake, two idealised setups were simulated: a macroscopic plant model in an ambient air flow and a microscopic model for the stomatal gas exchange. The simulations were done using the open source CFD code OpenFOAM (www.openfoam.com).

In the microscopic model the air flow was neglected and a pure diffusion process was simulated. Stomata were modelled as 100 µm long and 40 µm wide eye-shaped openings recessed 20 µm deep into the leaf surface. The simulation domain with 500 000 cells covered an area of 300 µm square around the stoma and extended 2 mm from the leaf surface into the surrounding gas. A single stoma with cyclic boundaries was used to represent a whole leaf with stomata spread repeatedly over its surface. The ozone-reactive bottom of the stomata was modelled as 100 % efficient sink (Laisk et al., 1989) with a constant ozone concentration of zero, while the side walls of the stomata were assumed not to absorb ozone and set to zero gradient. The top of the measurement domain acting as ozone inlet from the surrounding was set to one. The leaf surface around the stomata was set to zero gradient or to a fixed concentration of zero, representing two idealised plant types with either non-reactive or reactive leaf surface. “scalarTrans-





ACPD
15, 19873–19902, 2015



portFoam" was run on this grid with a uniform zero velocity field until a steady state was reached.

For the macroscopic model (see Supplement) a laminar flow around the plant was simulated using the steady state Reynolds averaged Navier–Stokes solver "simpleFoam", the transport of ozone in the resulting flow velocity field was studied using the "scalarTransportFoam" solver. The simulated gas volume consisted of a cube with 20 cm edge length with the shape of an exemplary tobacco plant cut out of its volume (see Fig. S4). The resulting simulation domain was divided into a hexahedron-dominant grid of 3.7 million cells with the finest granularity around the stomata and the leaf surfaces with the OpenFOAM tool "snappyHexMesh". The domain was divided into eight subdomains for parallel computation. Stomata were represented by small patches spread equally over the leaf surfaces, covering 10 % of the total leaf area. The boundary conditions for the gas flow simulation consisted of an inlet with 2 mm $s^{-1}$ velocity entering on one face of the cube and a constant pressure boundary condition outlet on the opposite face. The gas velocity on the plant surface was set to zero. Initial conditions for the flow simulation were calculated with "potentialFoam" to speed up convergence of the "simpleFoam" solver. The simulation was run until the flow velocity field reached a steady state. For the diffusion calculations a relative initial concentration of ozone was set to one at the inlet and to zero on the stomata patches. Like in the microscopic model calculations, the leaf surface was either a zero concentration gradient boundary for an idealised 3H02 plant type or a fixed concentration value of zero for an idealised *Ambalema* plant type. In the previously calculated velocity field the ozone transport was simulated until a steady state was reached, too.





ACPD
15, 19873–19902, 2015



## 3 Results and discussion

### 3.1 Detected oxidation products from plant surface ozonolysis of diterpenoids

We observed a prompt release of volatile carbonyls as soon as tobacco leaves were fumigated with ozone. The *Ambalema* and *Basma Drama* varieties released methyl vinyl ketone (MVK, $C_4H_6O$) and formaldehyde ($CH_2O$). These compounds are produced by surface-assisted ozonolysis of *cis*-abienol (see Figs. 1 and 2), a semi-volatile diterpenoid with two exocyclic double bonds. MVK was detected at $m/z$ 71.050 ($C_4H_7O^+$) and $m/z$ 100.040 ($C_4H_6O \cdot NO^+$) in the $H_3O^+$ respectively $NO^+$ reagent ion mode of the SRI-ToF-MS. Formaldehyde was detected only using $H_3O^+$ as reagent ion at $m/z$ 31.018 ($CH_3O^+$), taking into account the humidity dependent sensitivity (Hansel et al., 1997). In the $NO^+$ reagent ion mode formaldehyde can not be ionized (Španěl et al., 1997), consequently we detected no signal.

In addition, we detected sclaral, a non-volatile compound, in surface extracts obtained from fumigated *Ambalema* and *Basma Drama* plants (see Materials and methods and Supplement). Sclaral is an isomerisation product of the $C_{16}$ carbonyl formed in *cis*-abienol ozonolysis (cf. Fig. 1).

In the case of the ring structured CBTdiols with three endocyclic double bonds, produced by the *Basma Drama* and *BYBA* plants, at least two ozonolysis steps are needed to form volatile carbonyls (see Fig. 1). The most volatile ozonolysis product – 4-oxopentanal ($C_5H_8O_2$) – was detected by SRI-ToF-MS in the gas phase at $m/z$ 101.060 ($C_5H_9O_2^+$) in $H_3O^+$ and $m/z$ 99.045 ($C_5H_7O_2^+$) in $NO^+$ reagent ion mode, respectively.

According to the Criegee mechanism (Criegee, 1975), along with the carbonyls, Criegee Intermediates are also formed in ozonolysis reactions. However, they are expected to be too short-lived to be directly detected by the instruments used in our experiments (see Supplement).





ACPD
15, 19873–19902, 2015



### 3.2 Separation of ozone surface and gas phase reactions

The semi-volatile diterpenoids exuded by the tobacco varieties could also react with ozone in the gas phase. However, it is unlikely that gas phase reactions played a major role in our experiments. The air in the enclosure system was exchanged every ∼ 5 min. Therefore only extremely fast gas phase ozone – alkene reactions have to be considered. For an ozone concentration of 100 ppbv, a reaction rate of $1.35 \times 10^{-15}$ cm$^3$ s$^{-1}$ results in an alkene ozonolysis lifetime of 5 min. Such fast ozonolysis rates have only been measured for a few very reactive sesquiterpenes (Atkinson and Arey, 2003). We found no reaction rates of *cis*-abienol and CBTdiols with ozone in the literature to exclude the possibility of a gas phase contribution to total ozone loss in our experiments a priori. Nonetheless, taking into account the estimated vapour pressures of *cis*-abienol (∼ $10^{-9}$ bar) and CBTdiol (∼ $10^{-12}$ bar) (Goldstein and Galbally, 2007) we can state that the bulk of the exuded diterpenoids stayed at the leaf surface and that other surfaces (e.g. the inner surface of the plant enclosure and the tubing system) were very slowly covered by condensed diterpenoids. This is also the explanation for the bursts of volatile ozonolysis products at the beginning of every ozone fumigation (see e.g. Fig. 2). Diterpenoids were deposited on all surfaces during plant acclimation under ozone free conditions lasting for several hours (see also Supplement).

In order to assess the significance of gas phase ozonolysis to our results, we connected the plant enclosure containing a diterpenoid emitting tobacco plant with a second empty enclosure downstream and added ozone only to the second enclosure. Only negligible carbonyl signals were observed once the initial burst from deposited diterpenoids faded away (see Supplement and Fig. S1).

### 3.3 Ozonolysis of pure leaf surface compounds

In order to relate the release of carbonyls to surface chemistry only and to exclude stimulated emissions caused, e.g. by the plant ozone defence system, we investigated ozone reactions with pure leaf surface compounds. Leaf extracts were applied onto





ACPD
15, 19873–19902, 2015



the inner surface of an empty plant enclosure and fumigated with ozone the usual way (see Materials and methods section). *Ambalema* leaf extracts showed a weak signal of *cis*-abienol, which disappeared during ozone fumigation while MVK and formaldehyde were prominently observed. The *Basma Drama* extracts showed MVK, formaldehyde and 4-oxopentanal as ozonolysis products from *cis*-abienol and CBTdiols as expected. No significant amount of volatile carbonyls was observed from ozonolysis of 3H02 leaf extracts. Consistently, the total ozone conductance $g_{l,O_3}$ – a measure of the rate of ozone depleted at the surface – was far higher in experiments with extracts from diterpenoid-exuding tobacco varieties (see Fig. 3). This is in line with the results from the corresponding experiments with intact plants.

While the ozone depletion efficiency of the 3H02 exudates was decreasing fast, the presence of *cis*-abienol in *Ambalema* leaf exudates kept the ozone conductance at elevated levels for many hours (cf. Fig. 3). On fresh leaves of diterpenoid exuding tobacco varieties the total ozone conductance reached a steady state, when the diterpenoid production by the trichomes (leading to a permanent deposition of those onto the plant surface) and surface reactions were in equilibrium. Simulating diurnal ozone variations over two days in experiments with *Ambalema* and *Basma Drama* plants, we could show that the reactive layer at the plant surface is a large pool and not quickly consumed (see Supplement and Fig. S2). We therefore assume that the diterpenoids released represent a long term ozone protection.

### 3.4 Variety specific ozone depletion during dark and light phases

In order to have a measure of the ozone depletion capability of the various plants, the individual total ozone conductance $g_{l,O_3}$ was calculated (Caemmerer and Farquhar, 1981). At this point, $g_{l,O_3}$ is a measure of the rate of ozone depleted at the surface and within the stomata.

In dark experiments, when stomatal pores are almost closed, the *Ambalema* variety showed the highest total ozone conductance (cf. Fig. 4). This is a direct indication for the high ozone depletion capacity of the surface of this variety. Due to the lack of





ACPD
15, 19873–19902, 2015



reactive diterpenoids on the leaf surface of 3H02, the surface ozone sink plays a minor role for this tobacco line. However, we cannot totally exclude the presence of other unsaturated compounds at the surface of this tobacco line.

The low surface reactivity of the *Basma Drama* and *BYBA* varieties correlates with the lower amount of detected ozonolysis carbonyls compared to that of the *Ambalema* variety in dark conditions. This might be related to a lower diterpenoid surface coverage of these two varieties.

In a further step we investigated the change in total ozone conductance of different tobacco varieties when switching from dark to light conditions, thereby increasing stomatal conductance and thus stomatal ozone flux. Ozone entering the stomata is believed to be completely degraded (Laisk et al., 1989). In the case of *Ambalema*, switching the light on increased the total conductance by ∼ 55 % (see Fig. 4). In contrast, in the 3H02 case, switching on the light triggered a dramatic increase in the total ozone conductance by ∼ 340 % (cf. Fig. 4).

During light conditions the total ozone conductances of the different tobacco varieties were in a comparable range; slightly higher values were observed for the diterpenoid exuding lines *Ambalema*, *Basma Drama* and *BYBA*.

### 3.5 Fluid dynamic model calculations

Computational fluid dynamics calculations (see Materials and methods) revealed the principles responsible for this strong variety-dependent partitioning between stomatal and non-stomatal ozone loss. The mixed convective and diffusive ozone transport from the surrounding atmosphere to the plant surface and into the stomata was simulated for two idealised plant types under light conditions when the leaf stomata are open. The stomatal pores were exemplarily modelled as small patches uniformly spread over the entire leaf surface. For one model plant we assumed stomatal ozone uptake only, corresponding to an idealised 3H02 variety plant lacking any reactive surface compounds. The second model plant was representing an idealised *Ambalema* variety. The surface





ACPD
15, 19873–19902, 2015



acted as a perfect ozone sink with every ozone molecule reaching it being lost, either on the leaf surface or through the stomata.

Figure 5a and b show the resistance schemes used to describe the ozone flux to the leaves in the two scenarios, which were the basis for our simulations. Ambient ozone has to overcome the boundary layer resistance $R_b$ and the stomatal resistance $R_s$ before being destroyed in the stomatal cavity (for the sake of simplicity we neglected here the mesophyl resistance, which comprises diffusion through inner air spaces and dissolution of the gas in the cell wall water, followed by losses in the aqueous phase, penetration of plasmalemma or chemical reactions in the cell, cf. Neubert et al., 1993). In the case of a non-reactive leaf surface, ozone depletion within the stomata is the sole ozone sink (see Fig. 5a).

In the case of an ozone-reactive leaf surface, an additional surface chemical resistance $R_{sc}$ has to be introduced, which is parallel to the stomatal resistance (see Fig. 5b). $R_{sc}$ correlates with the reactive uptake coefficient of ozone at the leaf surface. In the case of the model plant having a non-reactive surface, $R_{sc}$ is very large ($R_{sc} \rightarrow \infty$) and ozone flux to the leaf surface can be omitted. Conversely, $R_{sc}$ is small for reactive surfaces.

The porous leaf surface architecture has special relevance for the gas uptake of plants. For gases having a negligible leaf surface sink (or source) – like e.g. $CO_2$ – steep concentration gradients parallel and perpendicular to the surface develop in close proximity to the stomata. These gradients enhance the gas transport in the diffusive leaf boundary layer towards the pores. This effect is extensively described in the literature as the "paradox of pores". It enables plants to effectively harvest $CO_2$ for photosynthesis, but in the same manner also "funnels" phytotoxic ozone through the stomata into the plant leaves (see Fig. 5c).

In the case of an ozone-reactive leaf surface, $R_{sc}$ is small compared to $R_s$ and only surface-parallel ozone concentration isosurfaces develop (black lines in Fig. 5d). Concentration gradients (white lines) close to the stomata are exclusively perpendicular to the surface. Consequently, the ozone transport in the diffusive leaf boundary layer





ACPD
15, 19873–19902, 2015



is equally distributed over the whole leaf surface and the ozone concentration in this layer is strongly reduced (see Fig. 5d). The surface-parallel concentration isosurfaces are also the reason why we can use the same reference concentration $c_{b,r}$ for both stomatal and surface chemical resistance, (cf. Fig. 5b). However, this approach does only hold if the leaf surface is a complete ozone sink (see Supplement and Fig. S3).

The different ozone concentration patterns in the two modelled scenarios have important implications for the stomatal ozone uptake. Typically, the stomatal conductance of ozone $g_{s,O_3}$ is estimated from that of water $g_{s,H_2O}$, by correcting for the different diffusivity of the two gases (see e.g. Neubert et al., 1993). The stomatal ozone flux $F_{s,O_3}$ can then be calculated with the following formula:

$$F_{s,O_3} = g_{s,O_3} \cdot (c_{i,O_3} - c_{b,O_3}) \quad (1)$$

with $c_{i,O_3}$ being the ozone concentration in the leaf intercellular space and $c_{b,O_3}$ the ozone concentration in the leaf boundary layer. $c_{i,O_3}$ is typically assumed to be close to zero (Laisk et al., 1989). Therefore, Eq. (1) simplifies to

$$F_{s,O_3} = -g_{s,O_3} \cdot c_{b,O_3} \quad (2)$$

If now surface reactions drastically reduce $c_{b,O_3}$ (cf. Fig. 5b), the effective stomatal ozone flux is reduced, too (unless extremely turbulent air conditions prevent the formation of an ozone depleted leaf boundary layer). Therefore, whenever surface loss plays a role, both surface and stomatal ozone uptake by plants have to be considered together. Previous studies might therefore have overestimated stomatal ozone uptake (e.g. Kurpius and Goldstein, 2003; Cieslik, 2004; Goldstein et al., 2004; Fares et al., 2012).

It is not correct to calculate stomatal ozone loss applying the resistance scheme shown in Fig. 5a and to eventually define the surface loss of ozone as that portion of the total loss which is not explainable by gas phase reactions and stomatal uptake. Due to the fact that surface reactions reduce $c_{b,O_3}$, surface loss has to be considered right from the beginning in order not to overestimate stomatal ozone uptake.





ACPD
15, 19873–19902, 2015



For obvious reasons this surface effect also has a consequence on the effective ozone dose which actually determines the phytotoxic effects of ozone (Massman, 2004). At this point, it is important to note that the uptake of non surface-reactive gases such as $CO_2$ is not affected by the altered ozone gradients.

For real plants this surface effect is less pronounced depending on stomata depth, which reduces the total stomatal uptake, and reactive surface compounds, which show smaller surface reaction rates than assumed for the idealised 100 % efficient ozone depleting surface (see Supplement). On the contrary, plants will hardly lack any reactive surface compounds, which explains why we observed a little ozone uptake during dark conditions also for the 3H02 variety, which has no significant diterpenoid emissions (cf. Fig. 4). Nonetheless, the simulations explain the experimentally observed behavior of different tobacco plants very well.

### 3.6 Atmospheric implications

Our results also have relevance for other ozone-initiated processes that occur in the outdoor environment. Semi-volatile, unsaturated organic species are common on various surfaces including soil with plant litter, aerosols, sea surface layers, man-made structures and plant surfaces. These are therefore potential sources of oxygenated VOC in ozone rich regions.

Resins, e.g. found at the surface of coniferous trees, contain high amounts of sesqui-, di- and triterpenoid compounds (Langenheim, 2003); triterpenoids are also a known constituent of surface waxes (Thimmappa et al., 2014). All these compound classes contain carbon-carbon double bonds and are therefore reactive with ozone. This could contribute to the varying ozone sensitivity of different conifer species (Schnitzler et al., 1999; Landolt et al., 2000) when exposed to the same cumulative ozone concentrations under light conditions. We anticipate therefore that surface ozonolysis plays an important role for the ozone tolerance of certain conifer species, too. Preliminary experiments with Norway spruce and Scots pine indeed point in this direction. However, due to the vast variety of different terpenoids present at the surface of these





ACPD
15, 19873–19902, 2015



species, the assignment of observed ozonolysis products to specific precursor compounds represents a challenge.

Additional support that surface ozonolysis might also be an important source of oxygenated VOC comes from field observations. Large downward ozone fluxes (Kurpius and Goldstein, 2003; Goldstein et al., 2004) and high levels of oxidized VOC (Holzinger et al., 2005) have been taken as evidence for "unconventional in-canopy chemistry" of unknown precursors in forest sites.

## 4 Conclusions

Our results reveal for the first time a powerful ozone protection mechanism of plants which takes place before the phytotoxic gas enters the stomata. Plants emitting unsaturated semi-volatile compounds could have a beneficial effect for neighbouring plants as well: either directly by reducing overall ozone concentrations (see Supplement) or indirectly through the deposition of the semi-volatile compounds onto unprotected neighbouring leaves.

Our findings have relevance not only for plants, but also for additional ozone-initiated processes that occur in the atmospheric boundary layer. The surface-assisted chemistry that we have elucidated for specific diterpenoids, linking for the first time volatile and non-volatile carbonyl products to semi-volatile precursors at the plant surface, is likely to occur also for other semi-volatile organic compounds on different surfaces (e.g. soil with plant litter, aerosols (Rogge et al., 1993), man-made structures and even human skin, as has been shown previously, Wisthaler and Weschler, 2010). Some of the ozonolysis-derived products may play important roles in atmospheric processes, influencing the budgets of OH radicals and ozone. Conversely, in our experiments we had no indication that surface ozonolysis itself releases detectable amounts of OH radicals into the gas phase (see Supplement). In order to assess the global impact of surface-assisted ozonolysis on atmospheric chemistry a more complete knowledge about the nature of reactive, semi- and low-volatility compounds at plant surfaces as well as the





ACPD
15, 19873–19902, 2015



mechanisms triggering their release (e.g. constitutive vs. biotic and mechanical stress induced emission) is needed.

## Appendix A: Generation of the 3H02 variety – a *Nicotiana tabacum* line without diterpenoids

The *Ambalema* variety which produces only *cis*-abienol and the *Colorado* variety which produces only CBTdiols (Sallaud et al., 2012) were crossed to produce hybrid F1 plants which produce both diterpenoids. Because the genetic loci responsible for the absence of CBTdiols and the absence of *cis*-abienol are distinct and unlinked, recombinant plants which produce neither diterpenoids could be recovered by analysing the leaf surface extracts by GC-MS in the selfed progeny of the F1 plants. One of these plants was selected, propagated over 2 generations by single seed descent and named line 3H02.

## Appendix B: Calculation of the total ozone conductance

For the calculation of the gas exchange parameters we followed well established procedures by Caemmerer and Farquhar (1981). Transpiration rate $E$, assimilation rate $A$ and ozone fluxes $F_{O_3}$ were calculated from

$$E = \frac{u_e}{s} \cdot \frac{w_o - w_e}{1 - w_o}, \ [\mathrm{mmol\,(m^2\,s)^{-1}}] \tag{B1}$$

$$A = \frac{u_e}{s} \cdot \left[ c_e - \left( \frac{1 - w_e}{1 - w_o} \right) \cdot c_o \right], \ [\mathrm{\mu mol\,(m^2\,s)^{-1}}] \tag{B2}$$

$$F_{O_3} = \frac{u_e}{s} \cdot \left[ o_e - \left( \frac{1 - w_e}{1 - w_o} \right) \cdot o_o \right], \ [\mathrm{nmol\,(m^2\,s)^{-1}}] \tag{B3}$$





ACPD
15, 19873–19902, 2015



with $u_e$ the molar flow of air entering the enclosure, $s$ the leaf area, $w_e/c_e/o_e$ and $w_o/c_o/o_o$ the mole fraction of water vapour/$CO_2$/ozone entering respectively leaving the plant enclosure.

For the calculation of the total ozone conductance we applied a ternary diffusion model as has been proposed by Caemmerer and Farquhar (1981). Thereby, pairwise interactions between ozone, water vapour and air are considered (for the sake of simplicity we neglected interactions with $CO_2$). Interactions of ozone molecules with water vapour are important only for that portion of ozone, which is entering the stomatal pores and not for that lost in reactions at the leaf surface. However, in the latter case the consideration of binary diffusion between ozone and water leads to an overestimation of the total ozone conductance in the range of < 1 %.

Total ozone conductance $g_{l,O_3}$ is then defined by

$$g_{l,O_3} = \frac{-F_{O_3} + \left(\frac{o_a+o_i}{2}\right)\cdot E}{o_a - o_i}, \ [\mathrm{mmol\,(m^2\,s)^{-1}}] \tag{B4}$$

with $o_i$ and $o_a$ the mole fractions of ozone inside the leaf (at the leaf surface for reactive leaf surfaces) and in the surrounding air, respectively. Typically, we consider $o_i \approx 0$ (Laisk et al., 1989) and therefore Eq. (B4) simplifies further to

$$g_{l,O_3} = \frac{-F_{O_3} + \frac{o_a}{2}\cdot E}{o_a} \tag{B5}$$

**The Supplement related to this article is available online at doi:10.5194/acpd-15-19873-2015-supplement.**

*Acknowledgements.* The authors would like to thank Francesco Loreto who initiated the tobacco experiments, Jörg-Peter (Jogi) Schnitzler for fruitful discussions and the gardeners of the Innsbruck University Botanic Gardens who grew the sample plants. W. Jud would like to thank Sheldon L. Cooper for helpful comments.





ACPD
15, 19873–19902, 2015



This project was financially supported by the European Science Foundation in the frame of the EuroVol MOMEVIP project and by the Austrian Fonds zur Förderung der wissenschaftlichen Forschung, project number I655-B16.

## References

Ashmore, M. R.: Assessing the future global impacts of ozone on vegetation, Plant Cell Environ., 28, 949–964, doi:10.1111/j.1365-3040.2005.01341.x, 2005. 19875

Atkinson, R. and Arey, J.: Atmospheric degradation of volatile organic compounds, Chem. Rev., 103, 4605–4638, doi:10.1021/cr0206420, 2003. 19884

Breitenlechner, M. and Hansel, A.: Development of an Advanced Selective Reagent Ionization Time of Flight Mass Spectrometer (advanced SRI-TOF-MS), Atmos. Meas. Tech. Discuss., submitted, 2015. 19878

Caemmerer, S. and Farquhar, G. D.: Some relationships between the biochemistry of photosynthesis and the gas exchange of leaves, Planta, 153, 376–387, doi:10.1007/BF00384257, 1981. 19885, 19891, 19892

Cape, J. N., Hamilton, R., and Heal, M. R.: Reactive uptake of ozone at simulated leaf surfaces: implications for "non-stomatal" ozone flux, Atmos. Environ., 43, 1116–1123, doi:10.1016/j.atmosenv.2008.11.007, 2009. 19875

Cieslik, S. A.: Ozone uptake by various surface types: a comparison between dose and exposure, Atmos. Environ., 38, 2409–2420, doi:10.1016/j.atmosenv.2003.10.063, 2004. 19875, 19888

Criegee, R.: Mechanism of ozonolysis, Angew. Chem. Int. Edit., 14, 745–752, 1975. 19883

Dentener, F., Stevenson, D., Ellingsen, K., Van Noije, T., Schultz, M., Amann, M., Atherton, C., Bell, N., Bergmann, D., Bey, I., Bouwman, L., Butler, T., Cofala, J., Collins, B., Drevet, J., Doherty, R., Eickhout, B., Eskes, H., Fiore, A., Gauss, M., Hauglustaine, D., Horowitz, L., Isaksen, I. S. A., Josse, B., Lawrence, M., Krol, M., Lamarque, J. F., Montanaro, V., Müller, J. F., Peuch, V. H., Pitari, G., Pyle, J., Rast, S., Rodriguez, J., Sanderson, M., Savage, N. H., Shindell, D., Strahan, S., Szopa, S., Sudo, K., Van Dingenen, R., Wild, O., and Zeng, G.: The global atmospheric environment for the next generation, Environ. Sci. Technol., 40, 3586–3594, doi:10.1021/es0523845, 2006. 19875





ACPD
15, 19873–19902, 2015



Enzell, C. R., Wahlberg, I., and Ryhage, R.: Mass spectra of tobacco isoprenoids, Mass Spectrom. Rev., 3, 395–438, doi:10.1002/mas.1280030304, 1984. 19881
Fahn, A.: Secretory tissues in vascular plants, New Phytol., 108, 229–257, doi:10.1111/j.1469-8137.1988.tb04159.x, 1988. 19876
Fares, S., Weber, R., Park, J.-H., Gentner, D., Karlik, J., and Goldstein, A. H.: Ozone deposition to an orange orchard: partitioning between stomatal and non-stomatal sinks, Environ. Pollut., 169, 258–266, doi:10.1016/j.envpol.2012.01.030, 2012. 19875, 19888
Felzer, B., Reilly, J., Melillo, J., Kicklighter, D., Sarofim, M., Wang, C., Prinn, R., and Zhuang, Q.: Future effects of ozone on carbon sequestration and climate change policy using a global biogeochemical model, Climatic Change, 73, 345–373, doi:10.1007/s10584-005-6776-4, 2005. 19875
Fruekilde, P., Hjorth, J., Jensen, N., Kotzias, D., and Larsen, B.: Ozonolysis at vegetation surfaces, Atmos. Environ., 32, 1893–1902, doi:10.1016/S1352-2310(97)00485-8, 1998. 19875
Goldstein, A. H. and Galbally, I. E.: Known and unexplored organic constituents in the Earth's atmosphere, Environ. Sci. Technol., 41, 1514–1521, doi:10.1021/es072476p, 2007. 19884
Goldstein, A. H., McKay, M., Kurpius, M. R., Schade, G. W., Lee, A., Holzinger, R., and Rasmussen, R. A.: Forest thinning experiment confirms ozone deposition to forest canopy is dominated by reaction with biogenic VOCs, Geophys. Res. Lett., 31, L22106, doi:10.1029/2004GL021259, 2004. 19875, 19888, 19890
Graus, M., Müller, M., and Hansel, A.: High resolution PTR-TOF: quantification and formula confirmation of VOC in real time, J. Am. Soc. Mass Spectr., 21, 1037–1044, doi:10.1016/j.jasms.2010.02.006, 2010. 19878
Hansel, A., Singer, W., Wisthaler, A., Schwarzmann, M., and Lindinger, W.: Energy dependencies of the proton transfer reactions, Int. J. Mass Spectrom., 167–168, 697–703, doi:10.1016/S0168-1176(97)00128-6, 1997. 19883
Hewitt, C. N., Kok, G. L., and Fall, R.: Hydroperoxides in plants exposed to ozone mediate air pollution damage to alkene emitters, Nature, 344, 56–58, doi:10.1038/344056a0, 1990. 19875
Holzinger, R., Lee, A., Paw, K. T., and Goldstein, U. A. H.: Observations of oxidation products above a forest imply biogenic emissions of very reactive compounds, Atmos. Chem. Phys., 5, 67–75, doi:10.5194/acp-5-67-2005, 2005. 19890





ACPD
15, 19873–19902, 2015



Jenkin, M. E. and Clemitshaw, K. C.: Ozone and other secondary photochemical pollutants: chemical processes governing their formation in the planetary boundary layer, Atmos. Environ., 34, 2499–2527, doi:10.1016/S1352-2310(99)00478-1, 2000. 19875

Karl, T., Hansel, A., Cappellin, L., Kaser, L., Herdlinger-Blatt, I., and Jud, W.: Selective measurements of isoprene and 2-methyl-3-buten-2-ol based on $NO^+$ ionization mass spectrometry, Atmos. Chem. Phys., 12, 11877–11884, doi:10.5194/acp-12-11877-2012, 2012. 19879

Kennedy, B. S., Nielsen, M. T., Severson, R. F., Sisson, V. A., Stephenson, M. K., and Jackson, D. M.: Leaf surface chemicals from *Nicotiana* affecting germination of *Peronospora tabacina* (adam) sporangia, J. Chem. Ecol., 18, 1467–1479, doi:10.1007/BF00993221, 1992. 19876

Kennedy, B. S., Nielsen, M. T., and Severson, R. F.: Biorationals from *Nicotiana* protect cucumbers against *Colletotrichum lagenarium* (Pass.) ell. & halst disease development, J. Chem. Ecol., 21, 221–231, doi:10.1007/BF02036653, 1995. 19876

Kurpius, M. R. and Goldstein, A. H.: Gas-phase chemistry dominates $O_3$ loss to a forest, implying a source of aerosols and hydroxyl radicals to the atmosphere, Geophys. Res. Lett., 30, 1371, doi:10.1029/2002GL016785, 2003. 19875, 19888, 19890

Laisk, A., Kull, O., and Moldau, H.: Ozone concentration in leaf intercellular air spaces is close to zero, Plant Physiol., 90, 1163–1167, 1989. 19881, 19886, 19888, 19892

Landolt, W., Bühlmann, U., Bleuler, P., and Bucher, J. B.: Ozone exposure–response relationships for biomass and root/shoot ratio of beech (*Fagus sylvatica*), ash (*Fraxinus excelsior*), Norway spruce (*Picea abies*) and Scots pine (*Pinus sylvestris*), Environ. Pollut., 109, 473–478, doi:10.1016/S0269-7491(00)00050-6, 2000. 19889

Langenheim, J. H.: Plant Resins: Chemistry, Evolution, Ecology, and Ethnobotany, Timber Press, Portland, Cambridge, 2003. 19889

Lin, Y. and Wagner, G. J.: Surface disposition and stability of pest-interactive, trichome-exuded diterpenes and sucrose esters of tobacco, J. Chem. Ecol., 20, 1907–1921, doi:10.1007/BF02066232, 1994. 19876

Massman, W. J.: Toward an ozone standard to protect vegetation based on effective dose: a review of deposition resistances and a possible metric, Atmos. Environ., 38, 2323–2337, doi:10.1016/j.atmosenv.2003.09.079, 2004. 19875, 19889

Müller, M., Mikoviny, T., Jud, W., D'Anna, B., and Wisthaler, A.: A new software tool for the analysis of high resolution PTR-TOF mass spectra, Chemometr. Intell. Lab., 127, 158–165, doi:10.1016/j.chemolab.2013.06.011, 2013. 19879





ACPD
15, 19873–19902, 2015



Neubert, A., Kley, D., Wildt, J., Segschneider, H., and Förstel, H.: Uptake of NO, $NO_2$ and $O_3$ by sunflower (*Helianthus annuus* L.) and tobacco plants (*Nicotiana tabacum* L.): dependence on stomatal conductivity, Atmos. Environ. A-Gen., 27, 2137–2145, doi:10.1016/0960-1686(93)90043-X, 1993. 19887, 19888

Rogge, W. F., Hildemann, L. M., Mazurek, M. A., Cass, G. R., and Simoneit, B. R. T.: Sources of fine organic aerosol. 4. Particulate abrasion products from leaf surfaces of urban plants, Environ. Sci. Technol., 27, 2700–2711, doi:10.1021/es00049a008, 1993. 19890

Sallaud, C., Giacalone, C., Töpfer, R., Goepfert, S., Bakaher, N., Rösti, S., and Tissier, A.: Characterization of two genes for the biosynthesis of the labdane diterpene Z-abienol in tobacco (*Nicotiana tabacum*) glandular trichomes, Plant J., 72, 1–17, doi:10.1111/j.1365-313X.2012.05068.x, 2012. 19876, 19881, 19891

Schnitzler, J. P., Langebartels, C., Heller, W., Liu, J., Lippert, M., Dohring, T., Bahnweg, G., and Sandermann, H.: Ameliorating effect of UV-B radiation on the response of Norway spruce and Scots pine to ambient ozone concentrations, Glob. Change Biol., 5, 83–94, doi:10.1046/j.1365-2486.1998.00208.x, 1999. 19889

Sitch, S., Cox, P. M., Collins, W. J., and Huntingford, C.: Indirect radiative forcing of climate change through ozone effects on the land-carbon sink, Nature, 448, 791–794, doi:10.1038/nature06059, 2007. 19875

Španěl, P., Ji, Y., and Smith, D.: SIFT studies of the reactions of $H_3O^+$, $NO^+$ and $O_2^+$ with a series of aldehydes and ketones, Int. J. Mass Spectrom., 165–166, 25–37, doi:10.1016/S0168-1176(97)00166-3, 1997. 19879, 19883

Thimmappa, R., Geisler, K., Louveau, T., O'Maille, P., and Osbourn, A.: Triterpene biosynthesis in plants, Annu. Rev. Plant Biol., 65, 225–257, doi:10.1146/annurev-arplant-050312-120229, 2014. 19889

Van Dingenen, R., Dentener, F. J., Raes, F., Krol, M. C., Emberson, L., and Cofala, J.: The global impact of ozone on agricultural crop yields under current and future air quality legislation, Atmos. Environ., 43, 604–618, doi:10.1016/j.atmosenv.2008.10.033, 2009. 19875

Vingarzan, R.: A review of surface ozone background levels and trends, Atmos. Environ., 38, 3431–3442, doi:10.1016/j.atmosenv.2004.03.030, 2004. 19875

Wagner, G. J.: Secreting glandular trichomes: more than just hairs, Plant Physiol., 96, 675–679, 1991. 19876





ACPD
15, 19873–19902, 2015



Wang, X. and Mauzerall, D. L.: Characterizing distributions of surface ozone and its impact on grain production in China, Japan and South Korea: 1990 and 2020, Atmos. Environ., 38, 4383–4402, doi:10.1016/j.atmosenv.2004.03.067, 2004. 19875

Wisthaler, A. and Weschler, C. J.: Reactions of ozone with human skin lipids: sources of carbonyls, dicarbonyls, and hydroxycarbonyls in indoor air, P. Natl. Acad. Sci. USA, 107, 6568–6575, doi:10.1073/pnas.0904498106, 2010. 19877, 19890

Wohlgemuth, H., Mittelstrass, K., Kschieschan, S., Bender, J., Weigel, H.-J., Overmyer, K., Kangasjarvi, J., Sandermann, H., and Langebartels, C.: Activation of an oxidative burst is a general feature of sensitive plants exposed to the air pollutant ozone, Plant Cell Environ., 25, 717–726, doi:10.1046/j.1365-3040.2002.00859.x, 2002. 19875





ACPD
15, 19873–19902, 2015



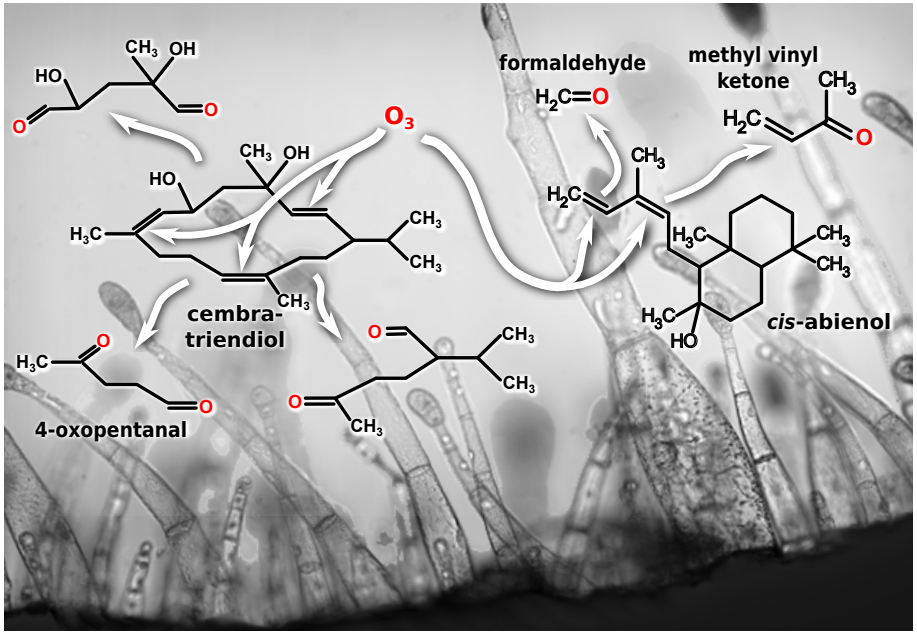


**Figure 1.** Ozonolysis of diterpenoids exuded by the trichomes of the investigated tobacco plants. The *BYBA* variety releases $\alpha$- and $\beta$-cembratriendiols ($C_{20}H_{34}O_2$), the *Ambalema* variety *cis*-abienol ($C_{20}H_{34}O$); the *Basma Drama* variety exudes all these compounds. Ozonolysis of the cembratriendiols requires at least two ozonolysis steps to form short-chained, volatile carbonyls, like e.g. 4-oxopentanal ($C_5H_8O_2$). Ozonolysis of *cis*-abienol leads to the formation of volatile formaldehyde ($CH_2O$) and methyl vinyl ketone ($C_4H_6O$).





ACPD
15, 19873–19902, 2015



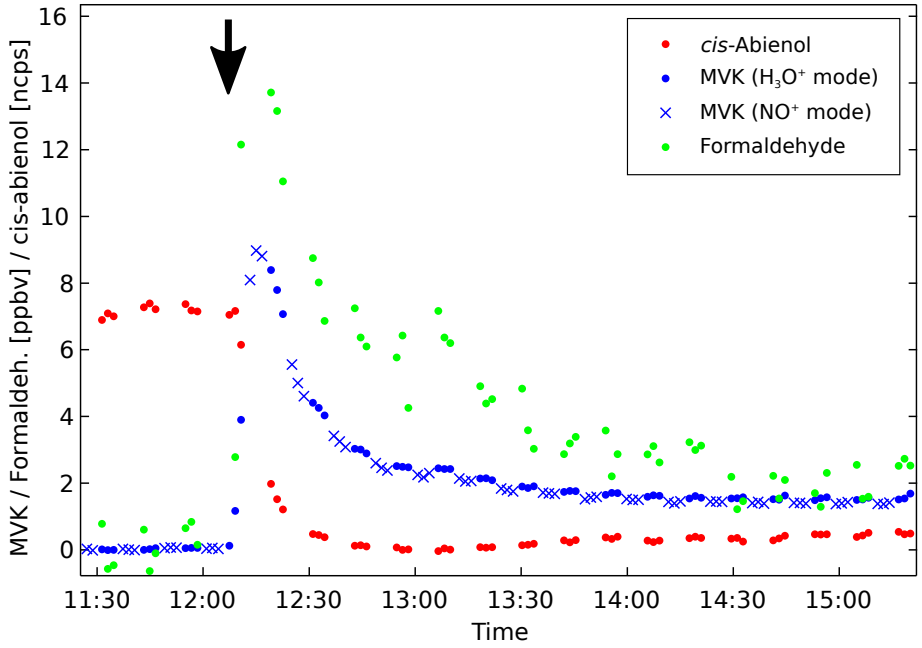


**Figure 2.** Temporal evolution of selected VOC in an ozonolysis experiment with an *Ambalema* plant. Starting the fumigation with ~ 60 ppbv ozone (indicated by the black arrow) the *cis*-abienol signal decreases quickly. At the same time, the carbonyl products of *cis*-abienol ozonolysis, formaldehyde and MVK (measured in $H_3O^+$ respectively $NO^+$ reagent ion mode of the SRI-ToF-MS), start to rise. The large scattering of the formaldehyde signal derives from the strongly reduced sensitivity of the SRI-ToF-MS under high humidity conditions towards this compound. Two hours after the start of the ozone fumigation an equilibrium between actual diterpenoid production and loss due to surface reactions is established, resulting in stable signals of the oxygenated VOC.





ACPD
15, 19873–19902, 2015



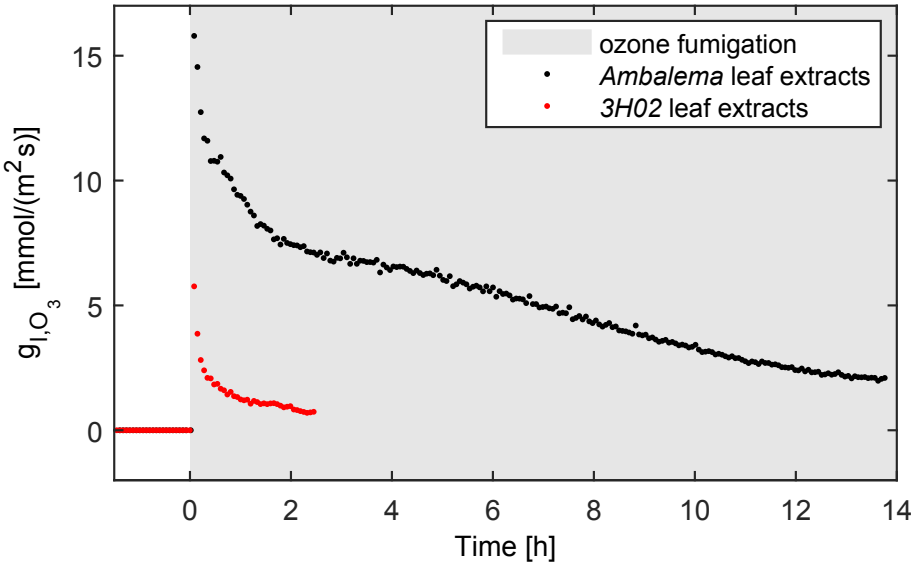


**Figure 3.** Ozonolysis experiments with pure leaf exudates extracted from non ozone fumigated, unimpaired plants. The leaf extracts containing the surface compounds were applied to the inner surface of the empty plant enclosure system (see Materials and methods section). During ozone fumigation (grey shaded area), the total ozone conductance $g_{I,O_3}$ to the enclosure surface was much higher for *Ambalema* leaf extracts than for 3H02 extracts. Moreover, it remained high for many hours.





ACPD
15, 19873–19902, 2015



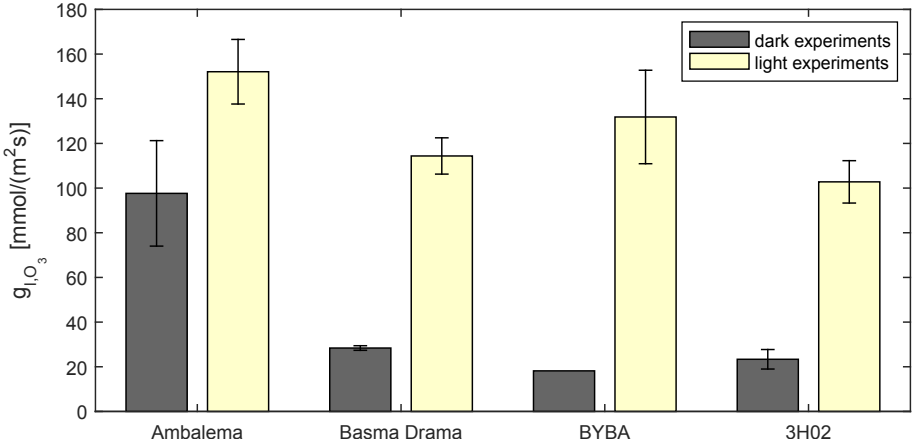


**Figure 4.** Total ozone conductance $g_{I,O_3}$ of different tobacco varieties during dark and light conditions. Error bars denote the standard error of 5 (13), 2 (6), 1 (5) and 3 (5) replicates of *Ambalema*, *Basma Drama*, *BYBA* respectively 3H02 in dark (light) experiments. Under dark conditions stomatal conductance is generally low and consequently surface reactions are the major ozone sink. The surface sink is high for the *Ambalema* tobacco line, which exudes *cis*-abienol and lower for the other lines, exuding less or no diterpenoids.





ACPD
15, 19873–19902, 2015



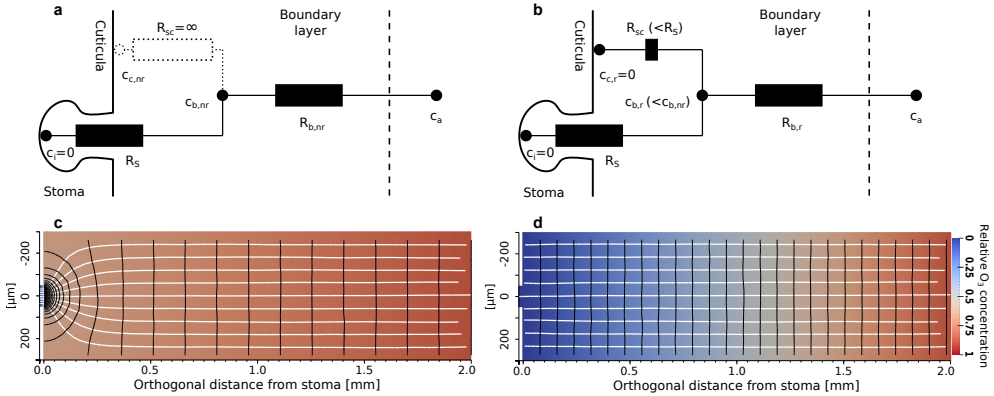


**Figure 5.** Fluid dynamic calculations of ozone uptake by stomata and leave surface. **(a** and **b)** show the resistance schemes for ozone uptake of leaves with non-reactive (nr) and reactive (r) surfaces. $c_i$, $c_c$, $c_b$ and $c_a$ denote ozone concentrations in the stomatal cavity, at the leaf surface, in the boundary layer and in ambient air, respectively. $R_s$ and $R_b$ denote the stomatal and boundary layer resistances. The surface chemical resistance $R_{sc}$ is infinite ($R_{sc} = \infty$) on a non-reactive surface. Fluid dynamic calculations reveal ozone concentration gradients (white lines indicate their orientation) evolving parallel and perpendicular to the leaf surface around the stoma (located at the coordinate (0,0)) in this case **(c)**. If the leaf surface is covered with ozone-reactive substances, the parallel fraction of the ozone gradients vanishes, resulting in isosurfaces of ozone concentration (black lines) parallel to the leaf surface and stronger ozone depletion in the leaf boundary layer **(d)**.





ACPD
15, 19873–19902, 2015